analytical chemistry

Article

pubs.acs.org/ac

New Spectral Deconvolution Algorithms for the Analysis of Polycyclic Aromatic Hydrocarbons and Sulfur Heterocycles by Comprehensive Two-Dimensional Gas Chromatography-Quadrupole Mass Spectrometery

Patrick M. Antle,[†] Christian D. Zeigler,[†] Yuriy Gankin,[‡] and Albert Robbat, Jr.*[,†]

[†]Tufts University Department of Chemistry, Medford, Massachusetts 02155, United States

[‡]Institute of Theoretical Chemistry, Inc., Needham, Massachusetts 02494, United States

ABSTRACT: New mass spectral deconvolution algorithms have been developed for comprehensive two-dimensional gas chromatography/quadrupole mass spectrometry (GC × GC/qMS). This paper reports the first use of spectral deconvolution of full scan quadrupole GC × GC/MS data for the quantitative analysis of polycyclic aromatic hydrocarbons (PAH) and polycyclic aromatic sulfur heterocycles (PASH) in coal tar-contaminated soil. A method employing four ions per isomer and multiple fragmentation patterns per alkylated homologue (MFPPH) is used to quantify target compounds. These results are in good agreement with GC/MS concentrations, and an examination of method precision, accuracy, selectivity, and sensitivity is discussed. MFPPH and SIM/1-ion concentration differences are also examined.

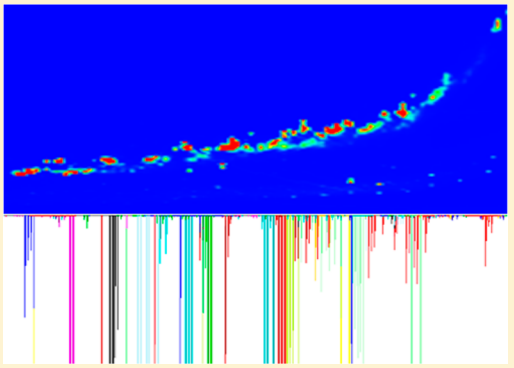

According to a recent publication,[1] tens of thousands of manufactured gas plant (MGP) sites worldwide require cleanup. For more than 100 years, the MGP industry produced coal tar as a waste product, and it continues to seep into the environment to this day. Its discharge is of primary importance, since coal tar moves in narrow seams long distances from its release point, with more mobile components traveling even longer distances. Coal tar is extremely complex, containing thousands of aliphatic, aromatic, asphaltenic, and polar compounds and resins, whose chemical entities span a wide range of physical and chemical properties.

How coal tar weathers in the environment is highly dependent on its surroundings,[2] with its composition differing from one location to the next, even within the same site.[3] Forensic scientists use polycyclic aromatic hydrocarbons (PAH), polycyclic aromatic sulfur heterocycles (PASH), and their alkylated homologues in soil and sediment to determine the degree of weathering that has occurred,[4] and toxicologists measure their concentrations in sediment, pore water, and benthic organisms to assess the risks posed to human health[5] and marine animals.[6] PAH, PASH, and their respective alkyl homologues serve, therefore, as useful forensic markers of environmental damage and their accurate, precise, sensitive, and selective measurement is of critical importance.

In previous work, we analyzed the aromatic fraction of fresh and weathered coal tar and crude oil samples by automated sequential gas chromatography/mass spectrometry (GC-GC/MS) to obtain the retention windows and fragmentation patterns for C_1−C_4 alkylated PAH.[7] We also determined the retention windows and fragmentation patterns for 119 parent and monoalkylated 2-, 3-, 4-, and 5-ring PASH archived by the National Institute of Standards and Testing (NIST).[8,9] From this work, we rationalized the fragmentation patterns for PAH and PASH isomers that cannot be found in either the literature or electronic databases. In addition to MS detection, a sulfur-specific, pulsed flame photometric detector confirmed fragmentation patterns were from PASH in the samples and, where possible, aligned with the fragmentation patterns produced by the reference compounds from NIST. This work, motivated by the high rates of false positives and overestimated concentrations produced by GC/MS methods that rely on too few ions to confirm compound identity, uses 3- to 5-ions per compound and as many fragmentation patterns as needed to identify all homologue isomers; hence, we call it multiple fragmentation patterns per homologue (MFPPH). We showed that homologue concentrations were significantly overestimated when the molecular ion or the molecular ion plus one confirming ion were used to determine target compound identity[7,8] and, in contrast, that C_2, C_3, and C_4 naphthalene concentrations were underestimated when one fragmentation pattern per homologue was used to identify isomers in coal tar- and oil-contaminated samples.[10]

Because automated sequential GC-GC/MS provides clean spectra of sample components in complex mixtures, it is ideal for building libraries. However, it is difficult to obtain quantitative data from this technique, since a single compound

Received: July 26, 2013
Accepted: September 24, 2013
Published: September 24, 2013

ACS Publications © 2013 American Chemical Society

can elute in more than one heart-cut and each heart-cut requires its own sample injection. Moreover, the amount transferred between columns is dependent on the modulation phase in relation to component position at time of sample transfer. Generally, separations on both columns must finish before subsequent injections occur, which results in impractically long analysis times for routine analytical work.

In this paper, we evaluate the data quality produced by new spectral deconvolution algorithms specifically developed for 2-dimensional GC × GC/MS. GC × GC is seen as the limiting case of GC-GC when the width of the heart-cut approaches zero,[11] offering multiple dimensions of separation on a far shorter time-scale than GC-GC.[12] The technique provides not only increased separation space and ease of visualization of sample components in complex mixtures,[13] but also improved sensitivity,[14] as "space compressed" second dimension peaks are up to 50-times narrower than first dimension peaks.[15]

Notwithstanding statistical overlap theory,[16] research has shown increases in separation capacity produced by GC × GC require compromise.[17] For example, suboptimal column conditions[17] and nonorthogonal stationary phases[18] impact peak capacity improvements.[19] Also, employing conventional mass spectrometry identification criteria requires reconciling the narrowness of the second dimension bandwidth with achieving sufficient invariant peak scans to correctly identify sample components. This can be problematic when low resolution mass filters, such as quadrupoles, are employed. Additionally, the modulation ratio (the number of sample portions transferred per first dimension peak)[20,21] and modulation phase (the sampling start time with respect to peak shape)[22] can alter detector signal, leading to quantitative errors.[14] When the effects of separation time on second dimension peak widths are ignored, longer modulation periods allow for increases in second column separation of coeluting compounds, but the correspondingly low modulation ratios lead to decreases in signal precision. In contrast, higher modulation ratios lead to increases in quantitative accuracy, but the correspondingly shorter modulation times limit the second dimension analysis time, which decreases separation capacity. Calculations show that by modifying separation and measurement attributes to obtain at least three modulations per first dimension peak, quality data is achievable.[14,17,21] Nonetheless, when isomers elute near enough to one another, their narrow, modulated peaks overlap such that spectral patterns of one compound are not discernible from others without spectral deconvolution.

While different mathematical and statistical models have been used in an attempt to deconvolve coeluting compounds in GC × GC/MS, these studies have used time-of-flight (TOF) mass filters and as such, have had the advantage of increased data density (mass spectra) across the peak compared to scanning quadrupole mass spectrometers (qMS).[23−25] For this reason, the use of a fast qMS with GC × GC is far less common. Only recently have researchers used this technique for quantitative analyses, including a semiquantitative study of coal tar-contaminated sediment.[26] Neither this investigation nor other GC × GC/TOF fingerprint[27] or classification[28] studies of coal tar have capitalized on the wealth of mass spectral information available in the data.

Spectral deconvolution of GC × GC/qMS data has not been published for coal tar or any other complex sample matrix. Despite significant differences in the number of data points produced by qMS and TOF analyzers, we believe quadrupole filters have advanced to produce sufficient peak scans so that low concentration analytes can be unambiguously identified when employing conventional mass spectrometry data analysis criteria. To test this hypothesis, a new spectral deconvolution algorithm was developed for GC × GC/qMS, which demonstrates that accurate, precise, selective, and sensitive measurements of PAH and PASH are achievable. Findings indicate the same quality of data is attainable by GC × GC/qMS as GC/qMS and on the same time scale, while providing the increased separation capacity and visual detail the technique is known for.

EXPERIMENTAL SECTION

Standards and Reagents. Airgas (Salem, NH) supplied the ultrahigh purity helium and nitrogen used in this study. The 16 EPA priority pollutant PAH, dibenzothiophene (DBT), and internal standards 1,4-dichlorobenzene-d_4, naphthalene-d_8, phenanthrene-d_{10}, chrysene-d_{12}, and perylene-d_{12} were purchased from Restek (Bellefonte, PA). A base/neutral surrogate spike mix (2-fluorobiphenyl, nitrobenzene-d_5, *p*-terphenyl-d_{14}) was purchased from Supelco (Bellefonte, PA) and chromatography-grade toluene and dichloromethane from Sigma-Aldrich (St. Louis, MO). PAH and dibenzothiophene (DBT) standards ranging from 0.001 to 25 μg/mL were prepared by serial dilution in dichloromethane.

Samples and Sample Preparation Procedure. A coal tar contaminated soil and bitumen tar sand were obtained from a utility in New York and from the Athabasca tar sand reservoir in Canada, respectively. For the coal tar soil, a borosilicate glass vial (Fisher Scientific, Pittsburgh, PA) containing 15 g of sample spiked with the surrogate mix and 8 mL of 50% by volume toluene/dichloromethane was sonicated (Branson Ultrasonics, Danbury, CT) for 10 min. This step was repeated 7-times to obtain maximum extraction efficiency. For the Athabasca tar sand, a 30 g sample was extracted in 30 mL of toluene using a CEM (Matthews, NC) Mars 6 microwave extraction unit. Activated copper and anhydrous sodium sulfate were used to eliminate elemental sulfur and water from the extracts, which were concentrated under a stream of nitrogen prior to the addition of internal standards. Calibration standards and samples were spiked with 1 μg/mL of the internal standard mixture.

Instrumentation. GC × GC/MS analyses were performed using an Agilent Technologies (Santa Clara, CA) 6890/5975C GC/MS with Gerstel (Mülheim an der Ruhr, Germany) MPS2 autosampler and CIS6 injector. Columns were connected using a Restek press-fit connector. The GC × GC cryogenic and thermal modulation hardware was obtained from Zoex Corporation (Houston, TX). GC Image (Lincoln, NE) supplied the software to create the three-dimensional chromatograms. Corresponding GC/MS analyses were performed using a Shimadzu (Columbia, MD) GC2010/QP2010+ instrument.

GC × GC/MS and GC/MS Analysis. The GC × GC/MS and GC/MS operating conditions are listed in Table S1. To establish measurement sensitivity, 1 μL of a serially diluted PAH and DBT standard was analyzed from 1 pg/μL to 25 ng/μL. The linear ranges and quantitation limits (LOQ) were determined, and the statistical limit of detection (LOD) was calculated using the student's *t*-test from the analysis of nine standards whose concentration was approximately one-half the LOQ. PAH and DBT response factors (RF) were calculated for each concentration over the dynamic range as follows: $A_X C_{IS}/$

$A_{IS}C_X$, where C_X is the analyte concentration and A_X its observed signal, with C_{IS} and A_{IS} the corresponding internal standard concentration and signal response. As discussed in our previous work,[29] a complete and accurate method would employ response factors for all fragmentation patterns, but due to a lack of existing standards, this is not possible. As such, in this study, alkylated PAH homologues were quantified using each parent's average RF. Additionally, alkyl PASH concentrations were calculated using the DBT response factor due to insufficient quantities of 4-ring parent PASH standards. These response factors only affect absolute concentrations, not the relative concentrations when comparing findings between MFPPH and single-ion analyses or between GC × GC/qMS and GC/qMS analyses, since the same alkylated PAH response factors were used independent of detection method.

Spectral deconvolution of GC/MS data was described in earlier work (Ion Analytics, Andover, MA).[18] For this study, new spectral deconvolution algorithms were developed to process GC × GC/MS data. The expressions below outline the identification process. A background signal for each PAH and PASH qualifier ion (in this case, the MFPPH ions) is subtracted from the peak signal. The reduced (relative to the base ion, $i = 1$) ion intensity, $I_i(t)$, at scan (t) is defined as follows:

$$I_i(t) = \frac{A_i(t)}{R_i A_1} \tag{1}$$

where $A_i(t)$ is the i-th qualifier ion intensity at scan (t) and R_i is the expected relative ion abundance ratio, which can be found in MS libraries such as NIST and Wiley or by analyzing standards. All qualifier ions are normalized to the base ion (for the base ion, $I_1 \equiv 1$). The spectral match, ΔI, is calculated by

$$\Delta I = \frac{\sum_{i=1}^{N-1} \sum_{j=i+1}^{N} Abs(I_i - I_j)}{\sum_{i=1}^{N-1} i} \tag{2}$$

where ΔI is the average relative reduced intensity deviation of each of the N qualifier ions. For each compound, the number of qualifier ions is selected by the analyst. In addition to the base ion, there should be at least two qualifier ions per compound. For this study, we used three ions for each parent compound and five ions per alkylated homologue fragmentation pattern.[8,10]

The closer ΔI is to zero, the better the match. In addition to this compound identity criterion, and to avoid inclusion of scans with skewed ion ratios, the scan-to-scan variance (SSV), ΔE, is calculated

$$\Delta E = \Delta I \cdot \log(A_1) \tag{3}$$

The target compound is considered present when the extracted ion ratios at scan (t) yield $\Delta E \leq \Delta E_{max}$, where the maximum allowable SSV is ΔE_{max}. Peak scans that fail this criterion are not included in the total peak area used to estimate analyte concentration in the sample. Another compound acceptance condition is

$$\Delta I \leq K + \frac{\Delta_0}{A_1} \tag{4}$$

where K is an acceptable percent relative difference selected by the analyst and Δ_0 is the additive error attributable to background (matrix) signal or instrument noise. This criterion measures both the ΔI at each scan and its variance from one scan to the next. If the intensity of a qualifier ion is higher than expected due to additive ion signal, the software compares all ion ratios against one another (computing a relative error for each peak scan) and will eliminate the signal from the matrix-affected ion if all other ions are in agreement (meaning ΔI is lower than the threshold value).

Target compound identity occurs when the ΔE or ΔI criterion is ≤7 in at least four consecutive peak scans. In addition, three other compound identity criteria must be met. First, the qualifier ratio deviation of the target ion must be $\leq u_i$ (the uncertainty value for the i-th confirming ion, e.g., ≤ 20%) at each scan in the peak. This criterion ensures that the spectra are invariant across the peak. Second, the Q-value must be ≥90. The Q-value is an integer between 1 and 100 that measures the deviation between the expected and observed ion ratios for each ion across the peak. The closer the Q-value is to 100, the higher the certainty that sample and library spectra match one another. Third, the Q-ratio must be ≤20% of the relative abundance. The Q-ratio is the peak area ratio of the extracted i-th and base ions. All of these criteria form a single acceptance condition. Only those scans that meet the above-mentioned criteria are selected for observation by the analyst, with the quantitative ion signal extracted from the peak and used to calculate A_X and A_{IS}. Given the multiple modulated peaks per compound, the deconvolution algorithms searched for up to twenty individual peaks per fragmentation pattern (or compound). For parent PAH, retention times were used to guide the search algorithms. For alkylated compounds, identification was based solely on spectral deconvolution.

RESULTS AND DISCUSSION

This study reports the first quantitative analysis of parent and alkyl PAH and PASH in coal tar by GC × GC/qMS. When compared to FID or TOF, significant operational trade-offs are required since qMS cannot approach the data collection rates of these detectors. Although SIM/1-ion detection has the potential of providing many more data points (peak-scans) than full-scan methods, we showed using too few ions leads to significant overestimation of alkylated PAH and PASH[8] in complex matrixes such as coal tar and crude oil and that accurate identification of target compounds requires at least three ions, whose relative abundances are within 20% of the known spectra, for at least four consecutive scans across the chromatographic peak.[30] Past research has shown that the spectrometer must produce at least seven scans per peak to obtain constant peak areas for quantitative analysis and that ion skewing, which hinders compound identification, was prevalent when six or fewer quadrupole peak scans were obtained; for example, five peak scans produced a 32% variation in the mass ratios.[31] Given the limitations of quadrupole technology, the stated goal of providing high quality quantitative data for these compounds in complex matrixes, and recognizing we could deconvolve comingled interfering ions from target spectra, we approached the method development problem as follows.

First, we addressed the need to achieve a minimum of three modulations per first dimension peak while avoiding peak wrap-around. Toward this end, some have employed slow temperature programs or lengthened columns to widen peaks. Instead, we used the same temperature program and column length as is typical for GC analysis, but with a much thicker first column stationary phase. Then, GC operating conditions and modulation periods were adjusted (Table S1) to optimize first column separation space and achieve three modulations

dx.doi.org/10.1021/ac402336j | Anal. Chem. 2013, 85, 10369−10376

Table 1. Ion Abundances and Calculated Relative Error for Each Scan Across One Modulated Acenaphthene Peak at One-Half of the Limit of Quantitation (LOQ)[a]

		scan number (time, min)						
ion (m/z)	expected abundance	21748 (26.978)	21749 (26.979)	21750 (26.980)	21751 (26.981)	21752 (26.982)	21753 (26.983)	21754 (26.984)
		relative abundance						
base (153)	100	100	100	100	100	100	100	100
qualifier 1 (154)	88	120	94	95	93	92	115	96
qualifier 2 (152)	45	50	50	48	48	52	61	ion missing
qualifier 3 (151)	17	18	18	17	17	19	21	ion missing
relative error		**19**	**4**	**3**	**2**	**3**	**18**	**failed criteria**

[a]Note: Eq 3 used to calculate relative error at each scan except 21754, which is missing confirming ions 151 and 152.

Table 2. GC×GC/MS Calibration and Regression Analysis

compound	range (ng/mL)[a]	$\overline{RF}$ (% RSD)[b]	slope ± SD	intercept ± SD	r^2	LOD (ng/g)[c]	spike (ng/g)[d]
naphthalene	10–3000	1.04 (11.3)	1.03 ± 0.08	0.00_3 ± 0.00_2	0.99	5.7	6
acenaphthylene	10–3000	1.19 (12.2)	1.25 ± 0.15	0.02 ± 0.02	0.99	10.7	12
acenaphthene	10–3000	1.09 (16.2)	0.99 ± 0.11	0.02 ± 0.02	0.99	5.7	6
fluorene	10–3000	0.65 (14.9)	0.71 ± 0.05	0.02 ± 0.02	1.00	7.5	6
dibenzothiophene	25–6000	0.68 (14.8)	0.71 ± 0.09	0.02 ± 0.02	1.00	19.3	24
phenanthrene/anthracene	10–3000	0.93 (10.1)	0.79 ± 0.16	0.03 ± 0.04	1.00	7.3	6
fluoranthene	10–3000	0.88 (15.4)	0.97 ± 0.18	0.02 ± 0.02	0.99	5.5	6
pyrene	10–3000	0.95 (12.0)	1.08 ± 0.19	0.02 ± 0.03	1.00	6.3	6
benzo(a)anthracene/chrysene	10–3000	1.10 (13.5)	0.98 ± 0.07	0.02 ± 0.01	0.99	22.3	24
benzo(b/k)fluoranthene	25–6000	0.73 (12.6)	1.13 ± 0.10	0.05 ± 0.04	0.99	13.5	12
benzo(a)pyrene	10–3000	0.74 (8.0)	0.88 ± 0.13	0.01 ± 0.01	0.99	17.7	24
indeno(1,2,3-c,d)pyrene	50–6000	0.76 (14.3)	0.70 ± 0.02	0.01 ± 0.01	1.00	34.2	24
dibenz(a,h)anthracene	50–6000	0.53 (12.3)	0.40 ± 0.20	0.00_1 ± 0.00	1.00	28.0	24
benzo(g,h,i)perylene	50–6000	0.76 (19.4)	0.61 ± 0.06	0.01 ± 0.01	1.00	35.8	24

[a]The low end of the concentration range is the LOQ. [b]The response factor was calculated at eight or more concentrations over the concentration range and then averaged. The $\overline{RF}$ was calculated from four different calibration curves produced over a 12 month period. [c]LOD was calculated from the student's t-test at ∼1/2 the LOQ. [d]Actual amount of PAH spiked into Athabasca tar sand extract.

Table 3. GC/MS Calibration and Regression Analysis

compound	range (ng/mL)[a]	RF (% RSD)[b]	slope	intercept	r^2	LOD (ng/g)[c]	spike (ng/g)[d]
naphthalene	200–25000	0.89 (10)	0.80	0.00_9	1.00	56.7	50
acenaphthylene	400–12500	1.18 (19)	1.52	0.06	0.99	69.8	50
acenaphthene	200–25000	0.86 (16)	0.95	0.00_4	1.00	24.3	25
fluorene	800–25000	0.92 (20)	1.19	0.09	0.99	171.0	100
dibenzothiophene	200–25000	0.77 (4)	0.82	0.01	1.00	91	100
phenanthrene	200–25000	0.88 (7)	0.92	0.02	0.99	26.5	25
anthracene	200–25000	0.60 (20)	0.84	0.05	0.99	78.0	50
fluoranthene	800–25000	0.80 (19)	1.02	0.08	0.99	92.5	100
pyrene	400–25000	0.88 (16)	1.08	0.05	1.00	105.4	100
benzo(a)anthracene	200–25000	0.75 (9)	0.83	0.01	1.00	88.7	100
chrysene	200–25000	0.75 (7)	0.83	0.02	0.99	86.4	100
benzo(b)fluoranthene	400–25000	0.70 (17)	0.81	0.01	0.99	185.0	200
benzo(k)fluoranthene	400–25000	0.74 (12)	0.83	0.02	0.99	125.9	100
benzo(a)pyrene	200–25000	0.75 (15)	0.91	0.04	0.99	102.0	100
indeno(1,2,3-c,d)pyrene	800–25000	0.76 (13)	0.86	0.06	0.99	149.1	100
dibenz(a,h)anthracene	800–25000	0.66 (18)	0.72	0.00_3	0.99	161.6	100
benzo(g,h,i)perylene	400–25000	0.79 (18)	0.97	0.04	0.99	117.1	100

[a]The low end of the concentration range is the LOQ. [b]The response factor was calculated at eight or more concentrations over the calibration range and then averaged. [c]LOD was calculated from the student's t-test at ∼1/2 the LOQ. [d]Actual amount of PAH spiked into Athabasca tar sand extract.

per first dimension peak, even for the least-retained PAH, naphthalene. The most-retained compound, benzo(*g*,*h*,*i*)-perylene, did not exhibit second dimension wrap-around under these conditions. The thicker-film column lowered the probability that highly impacted samples would overload the stationary phases and as a result, high concentration soil extracts were analyzed as prepared. In contrast, GC/MS analysis of the same samples on columns with 0.25 or 0.32 μm film thicknesses required dilution or split injection.

Second, we adjusted the chromatographic conditions to ensure second dimension peaks were as narrow as possible but with base-widths that yielded at least four consecutive scans/

dx.doi.org/10.1021/ac402336j | Anal. Chem. 2013, 85, 10369−10376

peak, which is the standard mass spectral peak identification criterion. Table 1 lists the relative abundances and the relative error (RE) calculated by eq 3 for each scan across a modulated acenaphthene peak at one-half of the LOQ. While scans 21749 to 21752 easily meet the RE criterion, ≤7, the relative error in scans 21748, 21753, and 21754, due to mass ratio skewing, missing ions, or interfering ions, exceed this criterion and are discarded; neither marked as acenaphthene nor included in peak area calculations.

To further assess qMS performance under GC × GC conditions, based on the criteria described in the Experimental Section, we calculated the ion ratio relative standard deviation (RSD) for the 16 PAH at both the midpoint of the calibration curve and the LOQ. The RSD was, on average, 7%. We also examined peak area precision and found that at one-half the LOQ, the qMS produced four consecutive scans that met the identification criteria and peak area RSD of <15%. In contrast, concentrations at the LOQ for each PAH produced at least six scans per peak, and for all concentrations in the linear portion of the calibration curve, the peak area RSD was 5%, which is excellent.

Tables 2 and 3 list the DBT and PAH calibration ranges, regression analyses, LOQ, LOD, and matrix spike results. Under the conditions employed, second dimension peaks of structural isomers such as phenanthrene and anthracene, benzo(a)anthracene and chrysene, and benzo(b and k)-fluoranthene overlap. As a result, first dimension peak separations become large groupings of modulated peaks whose spectra are indistinguishable. For these compounds, the reported data is the average of the signals for each isomer pair. For GC × GC/MS, the calibration curve produced average response factors (RF), relative standard deviations, and correlation coefficients (r^2) in agreement with those obtained by GC/MS. Moreover, measurement precision was <20%. This data was produced from four calibration curves over a 12-month period, highlighting the robustness of the data. It is understood that operation of the qMS in full-scan mode limits measurement sensitivity compared to SIM/1-ion and 2-ion methods, but it ensures accurate identification of target compounds. Nonetheless, the combination of a thicker first dimension stationary phase and higher signals due to peak modulation improved measurement sensitivity by 30-fold compared to GC/MS.

To evaluate whether LOQ concentrations were detectable in complex matrixes, an Athabasca tar sand, which is predominately aliphatics, resins, and asphaltenes, was spiked with known concentrations of PAH at one-half LOQ. This concentration approximates the LOD obtained from the statistical analysis of nine replicate samples. The respective matrix spiked concentrations were detectable using both GC × GC/MS and GC/MS, proving the deconvolution software can accurately identify and quantify target compounds independent of the matrix. This result is not possible using conventional data analysis software when additive ion currents from coeluting target and matrix compounds lead to distorted ion ratios.[18,32,33]

Figure 1 shows the GC × GC/MS chromatogram of coal tar-contaminated sediment from the Hudson River. This sample, representative of coal tar exposed to the environment for decades, is highly weathered and has lost some alkylated PAH and PASH due to evaporation, dissolution and microbial degradation. The total ion current (TIC) chromatogram is shown in Figure 2 (top). The bottom figure is the deconvolved reconstructed ion current (RIC) chromatogram of the parent

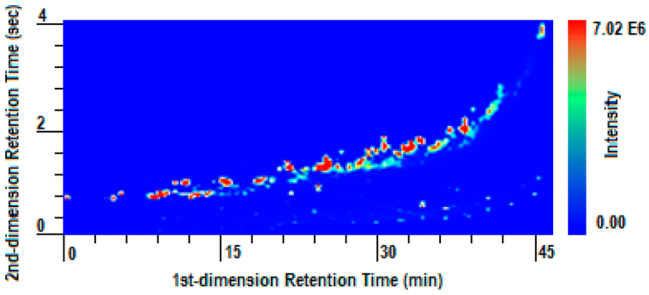

Figure 1. GC × GC/MS chromatogram of a weathered coal tar sediment.

and alkyl PAH and PASH. The deconvolution software automatically integrates the peak areas and for those homologues where multiple fragmentation patterns are needed to capture all isomers, it integrates and sums peaks by pattern. Figure 3 is an expanded view of the C_4-phenanthrene GC × GC/MS and GC/MS ion traces for the same sample. The dialogue box shows the ions, their relative abundances for one fragmentation pattern, and corresponding ion trace color. The dialogue box also shows the acceptance criteria that must be met as well as the number of potential peaks. The top chromatogram displays 10 modulated GC × GC/MS peaks, whereas the bottom chromatogram shows two GC/MS peaks for this pattern. The deconvolved ion signal at each peak scan is shown in the figure. When the ion signals meet the compound identity criterion for a given scan, the normalized ion currents are depicted in the form of a histogram for ease of visualization. A magnified view is shown for both GC × GC/MS and GC/MS data. After the ion signals are normalized, only those signals that appear at the same height (±20%) at a given scan and meet the scan-to-scan acceptance criteria are in the histogram. Scans that fail the acceptance criteria are neither integrated nor shown in the histogram, see example above. All GC × GC/MS peaks shown in the figure meet the compound acceptance criteria. In contrast, of the four GC/MS peaks in the center of the chromatogram, only the two outside peaks meet the acceptance criteria for the fragmentation pattern shown in the dialogue box. The two middle peaks do not, as only two of the three ions comaximize, making clear these peaks are not C_4-phenanthrenes.

PAH and PASH concentrations in the sediment sample shown in Figure 1 were measured by both GC × GC/MS and GC/MS to assess data quality differences. The U.S. Environmental Protection Agency (EPA) benchmark for accuracy is contingent on the site-specific action levels (AL) required to clean hazardous waste sites.[34,35] If we assume the site is adjacent to residential properties, the concentrations in the sample must meet the relative percent difference (RPD) shown in Table 4.[36,37] Parent PAH concentrations are well within EPA criteria for accuracy, and although homologue specific action levels are not reported, results are in excellent agreement and meet the same criteria as parent PAH. Some homologues exceed the low concentration benchmark, presumably due to sensitivity differences, while others are only detected by GC × GC/MS.

Since GC × GC/MS offers improved separation space and the corresponding ability to separate target compounds from matrix interferences, we examined if homologue identification employing too few ions still produced overestimated concentrations as reported in our previous studies. The same

dx.doi.org/10.1021/ac402336j | Anal. Chem. 2013, 85, 10369−10376

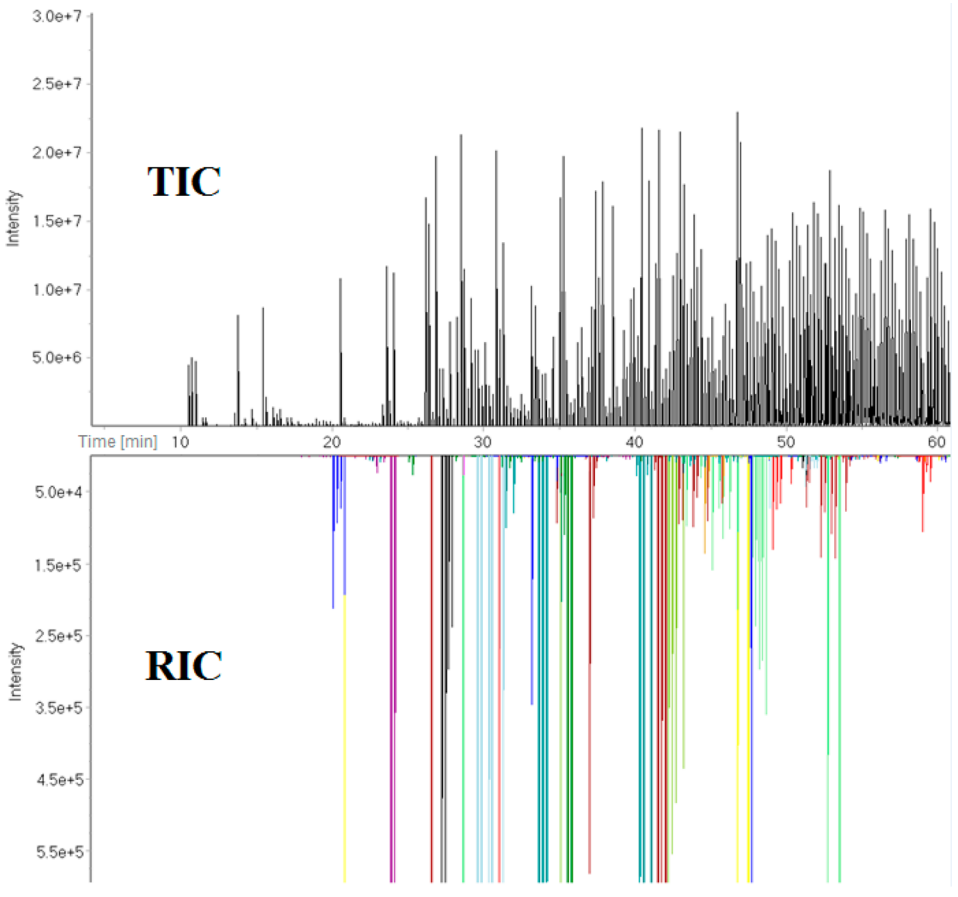

Figure 2. Total and reconstructed ion current (TIC/RIC) chromatograms of the coal tar soil sample shown in Figure 1

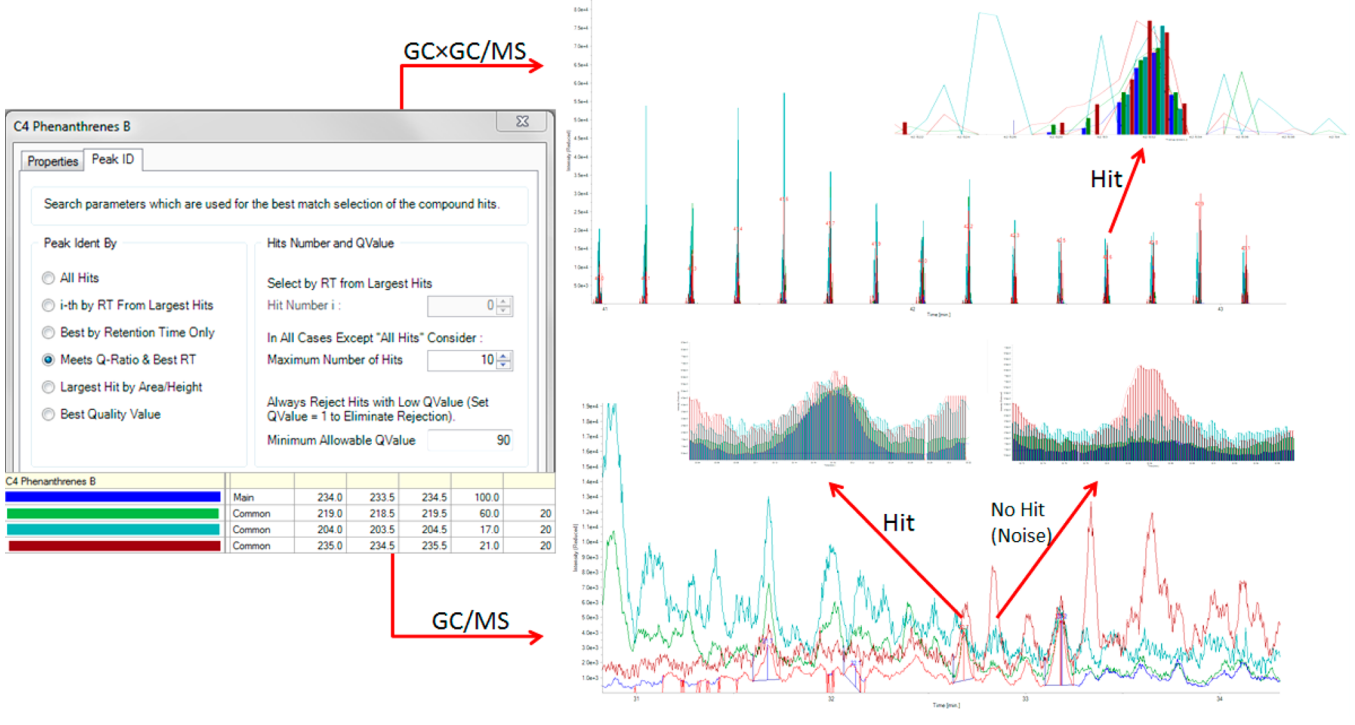

Figure 3. Illustrative example of spectral deconvolution of GC/MS and GC × GC/MS data of the coal tar soil shown in Figures 1 and 2

data file was analyzed by extracting the molecular ion signal (SIE, single ion extraction) and MFPPH ions of each homologue. Table 5 lists the concentration differences. SIE significantly overestimated 10 of 20 alkylated PAH and 10 of 15

dx.doi.org/10.1021/ac402336j | *Anal. Chem.* 2013, 85, 10369−10376

Table 4. PAH and PASH Concentrations in a Coal Tar Contaminated Soil Analyzed by GC×GC/MS and GC/MS Using the MFPPH Data Analysis Method

compound/ homologue	GC × GC/ MS (μg/g)	GC/MS (μg/g)	% RPD	2.5 × AL (μg/g) and[a](RPD)
naphthalene	0.7	0.7	0	5 (100)
C_1 naphthalenes	8.0	10	−20	
C_2 naphthalenes	15	19	−21	
C_3 naphthalenes	11	11	0	
C_4 naphthalenes	4.4	2.1	110	
fluorene	25	23	9	35 (100)
C_1 fluorenes	24	21	14	
C_2 fluorenes	13	9.7	34	
C_3 fluorenes	2.9	0.8	263	
C_4 fluorenes	1.6	ND	N/A	
phenanthrene/ anthracene	93	84	11	355 (100)
C_1 phenanthrenes	78	87	−10	
C_2 phenanthrenes	20	24	−17	
C_3 phenanthrenes	5.5	6.8	−19	
C_4 phenanthrenes	1.3	0.5	160	
benzo(a) anthracene/ chrysene	29	34	−15	0.25 (60)
C_1 chrysenes	27	37	−27	
C_2 chrysenes	3.0	3.3	−9	
C_3 chrysenes	0.8	ND	N/A	
C_4 chrysenes	ND	ND	N/A	
pyrene/ fluoranthene	73	72	1	262.5 (100)
C_1 pyrenes	61	76	−20	
C_2 pyrenes	17	22	−23	
C_3 pyrenes	4.2	1.9	121	
C_4 pyrenes	1.1	ND	N/A	
C_1 2-ring PASH	2.0	2.3	−13	
C_2 2-ring PASH	3.6	4.3	−16	
C_3 2-ring PASH	4.3	4.7	−9	
C_4 2-ring PASH	1.4	1.3	8	
dibenzothiophene	22	20	10	
C_1 3-ring PASH	30	29	3	
C_2 3-ring PASH	22	19	16	
C_3 3-ring PASH	9.7	7.3	33	
C_4 3-ring PASH	1.9	0.6	217	
C_1 4-ring fused PASH	17	14	21	
C_2 4-ring fused PASH	7.3	6.6	11	
C_3 4-ring fused PASH	0.7	ND	N/A	
C_4 4-ring fused PASH	0.6	0.8	−25	
C_1 4-ring condensed PASH	7.3	6.1	20	
C_2 4-ring condensed PASH	3.5	3.2	9	
C_3 4-ring condensed PASH	6.7	6.0	12	

[a]The relative percent difference (RPD) must be ≤60% or ≤100% when sample concentrations are greater than or less than 2.5-times the site-specific AL, respectively.[35]

Table 5. PAH and PASH Concentrations in a Coal Tar Contaminated Soil[a]

compound/homologue	MFPPH (μg/g)	SIE (μg/g)	overestimation (%)[b]
C_1 naphthalenes	8.0	8.0	0
C_2 naphthalenes	15	15	0
C_3 naphthalenes	11	11	0
C_4 naphthalenes	4.4	4.4	0
C_1 fluorenes	24	40	67
C_2 fluorenes	13	24	85
C_3 fluorenes	2.9	14	383
C_4 fluorenes	1.6	9.6	500
C_1 phenanthrenes	78	82	5
C_2 phenanthrenes	20	22	10
C_3 phenanthrenes	5.5	7.4	35
C_4 phenanthrenes	1.3	4.6	254
C_1 chrysenes	27	27	0
C_2 chrysenes	3.0	3.5	17
C_3 chrysenes	0.8	0.9	13
C_4 chrysenes	ND	ND	N/A
C_1 pyrenes	61	87	43
C_2 pyrenes	17	24	41
C_3 pyrenes	4.2	16	281
C_4 pyrenes	1.1	2.8	155
C_1 2-ring PASH	2.0	2.0	0
C_2 2-ring PASH	3.6	4.7	31
C_3 2-ring PASH	4.3	5.8	35
C_4 2-ring PASH	1.4	3.4	143
C_1 3-ring PASH	30	30	0
C_2 3-ring PASH	22	23	5
C_3 3-ring PASH	9.7	26	168
C_4 3-ring PASH	1.9	3.1	63
C_1 4-ring fused PASH	17	20	18
C_2 4-ring fused PASH	7.3	10	37
C_3 4-ring fused PASH	0.7	20	2757
C_4 4-ring fused PASH	0.6	1.0	67
C_1 4-ring condensed PASH	7.3	12	64
C_2 4-ring condensed PASH	3.5	7.9	126
C_3 4-ring condensed PASH	6.7	6.7	0

[a]The same GC×GC/MS data file was analyzed by MFPPH and SIE. [b] % overestimation = [(SIE − MFPPH)/MFPPH].

PASH homologues compared to MFPPH. The high positive bias ranged from thirty to thousands of percent and is consistent with our previous findings.[30] These results further substantiate our contention that identification, and thus quantitation, is subject to matrix bias when too few ions are used to differentiate homologue signals from matrix signals.

Our findings demonstrate quadrupole mass spectrometers can produce sufficient invariant scans to obtain high quality GC × GC data as measured by precision, accuracy, and sensitivity, with spectral deconvolution of MFPPH ions the key to obtaining selective compound detection in complex samples. This is especially important since many of the alkylated PAH and PASH elute within the same retention windows.[30] In addition to the 3-D image normally obtained by GC × GC, the deconvolved RIC traces increase analyst confidence that 3-D peaks are correctly assigned. Based on the findings above, we believe spectral deconvolution of GC × GC/qMS data can help to solve the vexing challenges inherent in complex mixture analysis.

AUTHOR INFORMATION

Corresponding Author

*E-mail: Albert.Robbat@Tufts.edu.

Notes

The authors declare the following competing financial interest(s): Albert Robbat is a principal in Ion Analytics, the provider of the spectral deconvolution software used in this study.

■ ACKNOWLEDGMENTS

The authors appreciate the support of Zoex, Gerstel, Shimadzu and Agilent for the instrumentation used in this study and Ion Analytics for the deconvolution software. The authors further appreciate the work of Eugene Baydakov (Institute of Theoretical Chemistry, Inc.) for coding the software.

■ REFERENCES

(1) Hatheway, A. W. *Remediation of Former Manufactured Gas Plants and Other Coal-Tar Sites*; CRC Press: Boca Raton, FL, 2011.
(2) Yim, U. H.; Kim, M.; Ha, S. Y.; Kim, S.; Shim, W. J. *Environ. Sci. Technol.* **2012**, *46*, 6431−6437.
(3) Wardlaw, G. D.; Nelson, R. K.; Reddy, C. M.; Valentine, D. L. *Org. Geochem.* **2011**, *42*, 630−639.
(4) Tobiszewski, M.; Namieśnik, J. *Environ. Pollut.* **2012**, *162*, 110−119.
(5) Mahler, B. J.; Metre, P. C. V.; Crane, J. L.; Watts, A. W.; Scoggins, M.; Williams, E. S. *Environ. Sci. Technol.* **2012**, *46*, 3039−3045.
(6) *Methods for the Derivation of Site-Specific Equilibrium Partitioning Sediment Guidelines (ESGs) for the Protection of Benthic Organisms: Non-ionic Organics*; EPA/822/R/02/042; US Environmental Protection Agency, Office of Science and Technology: Washington, DC, 2004.
(7) Zeigler, C. D.; Robbat, A., Jr. *Environ. Sci. Technol.* **2012**, *46*, 935−3942.
(8) Zeigler, C. D.; Wilton, N. D.; Robbat, A., Jr. *Anal. Chem.* **2012**, *84*, 2245−2252.
(9) Zeigler, C. D.; Schantz, M. M.; Wise, S.; Robbat, A., Jr. *Polycyclic Aromat. Compd.* **2012**, *32*, 154−176.
(10) Zeigler, C. D.; MacNamara, K.; Wang, Z.; Robbat, A., Jr. *J. Chrom. A* **2008**, *1205*, 109−116.
(11) Gorecki, T.; Harynuk, J. J.; Panic, O. *J. Sep. Sci.* **2004**, *27*, 359−379.
(12) De-Geus, H.; de Boer, J.; Brinkman, U. *TrAC − Trend. Anal. Chem.* **1996**, *15*, 168−178.
(13) Bertsch, W. *J. High Res. Chromatog.* **2000**, *23*, 167−181.
(14) de la Mata, A. P.; Harynuk, J. J. *Anal. Chem.* **2012**, *84*, 6646−6653.
(15) Beens, J.; Boelens, H.; Tijssen, R.; Blomberg, J. *J. High Res. Chromatog.* **1998**, *21*, 47−54.
(16) Davis, J. M. *Anal. Chem.* **1991**, *63*, 2141−2152.
(17) Blumberg, L. M.; David, F.; Klee, M. S.; Sandra, P. *J. Chromatogr., A* **2008**, *1188*, 2−16.
(18) Robbat, A., Jr; Kowalsick, A.; Howell, J. *J. Chromatogr., A* **2011**, *1218*, 5531−5541.
(19) Blumberg, L.; Klee, M. S. *J. Chromatogr., A* **2010**, *1217*, 99−103.
(20) Schoenmakers, P. J.; Marriott, P. J.; Beens, J. *LCGC Eur.* **2003**, *16*, 335−339.
(21) Harynuk, J. J.; Kwong, A. H.; Marriott, P. J. *J. Chromatogr., A* **2008**, *1200* (1), 17−27.
(22) Davis, J. M.; Stoll, D. R.; Carr, P. W. *Anal. Chem.* **2008**, *80*, 461−473.
(23) Mohler, R. E.; Tu, B. P.; Dombek, K. M.; Hoggard, J. C.; Young, E. T.; Synovec, R. E. *J. Chromatogr., A* **2008**, *1186*, 401−411.
(24) Zeng, Z.-D.; Chin, S.-T.; Hugel, H. M.; Marriott, P. J. *J. Chromatogr., A* **2011**, *1218*, 2301−2310.
(25) de Rijk, T. C.; Mol, H. G. J.; Punt, A.; van der Kamp, H.; van der Lee, M.; van der Weg, G. *J. AOAC Int.* **2011**, *94*, 1722−1740.
(26) Vasilieva, V.; Scherr, K. E.; Edelmann, E.; Hasinger, M.; Loibner, A. P. *J. Biotechnol.* **2012**, *157*, 460−466.
(27) McGregor, L. A.; Gauchotte-Lindsay, C.; Daeid, N. N.; Thomas, R.; Daly, P.; Kalin, R. M. *J. Chromatogr., A* **2011**, *1218*, 4755−4763.
(28) Gauchotte-Lindsay, C.; Richards, P.; McGregor, L. A.; Thomas, R.; Kalin, R. M. *J. Chromatogr., A* **2012**, *1253*, 154−163.
(29) Zeigler, C.; MacNamara, K.; Wang, Z.; Robbat, A., Jr *J. Chromatogr., A* **2008**, *1205*, 109−116.
(30) Antle, P. M.; Zeigler, C. D.; Wilton, N. M.; Robbat, A. *Int. J. Environ. Anal. Chem.* **2013**, DOI: 10.1080/03067319.2013.840886.
(31) Adahchour, M.; Brandt, M.; Baier, H.-U.; Vreuls, R. J. J.; Batenburg, A. M.; Brinkman, U. A. T. *J. Chromatogr., A* **2005**, *1067*, 245−254.
(32) Robbat, A., Jr.; Hoffmann, A.; MacNamara, K.; Huang, Y. *J. AOAC Int.* **2008**, *91*, 1467−1477.
(33) Robbat, A., Jr.; Smarason, S.; Gankin, Y. V. *Field Anal. Chem. Technol.* **1999**, *3*, 55−66.
(34) *Region 1 EPA-NE Data Validation Functional Guidelines for Evaluating Environmental Analyses*, Part II, Section VOA/SV−IX; U.S. Environmental Protection Agency, Office of Science and Technology: Washington, DC, 1996.
(35) *Supplemental Guidance for Developing Soil Screening Levels for Superfund Sites: Appendix A*, OSWER No. 9355.4-24; U.S. Environmental Protection Agency, Office of Science and Technology: Washington, DC, 2002.
(36) Robbat, A., Jr.; Considine, T.; Antle, P. M. *Chemosphere* **2010**, *80*, 1370−1376.
(37) Considine, T.; Robbat, A., Jr. *Environ. Sci. Technol.* **2008**, *42*, 1213−1220.